ARTICLE IN PRESS

Mechanics of Materials xxx (2015) xxx–xxx

Contents lists available at ScienceDirect

Mechanics of Materials

journal homepage: www.elsevier.com/locate/mechmat

Atomistic insights into Li-ion diffusion in amorphous silicon

Xin Yan [a], Afif Gouissem [a], Pradeep Sharma [a,b,c,*]

[a] Department of Mechanical Engineering, University of Houston, Houston, TX 77004, USA
[b] Department of Physics, University of Houston, Houston, TX 77004, USA
[c] Materials Science and Engineering Program, University of Houston, Houston, TX 77004, USA

ARTICLE INFO

Article history:
Received 30 December 2014
Received in revised form 8 March 2015
Available online xxxx

Keywords:
Li
Diffusion
Potential landscape
Autonomous basin climbing (ABC)

ABSTRACT

Silicon has been critically examined for its potential use as an electrode material for Li-ion batteries. Diffusive transport of Li-ions in the crystalline silicon anode is one of the key mechanisms that controls the deformation during lithiation, the rate of the charge–discharge cycle, and eventual mechanical failure. The use of amorphous silicon, instead of its crystalline counterpart, is considered to offer several advantages. The atomistic mechanisms underpinning diffusive transport of Li-ions in amorphous silicon are, however, poorly understood. Conventional molecular dynamics, if used to obtain atomistic insights into the Li-ion transport mechanism, suffers from several disadvantages: the relaxation times of Li ion diffusion in many of the diffusion pathways in amorphous Si are well beyond the short time scales of conventional molecular dynamics. In this work we utilize a sequence of approaches that involve the employment of a novel and recently developed potential energy surface sampling method, kinetic Monte Carlo, and the transition state theory to obtain a realistic evaluation of Li-ion diffusion pathways in amorphous Si. Diffusive pathways are not *a priori* set but rather emerge naturally as part of our computation. We elucidate the comparative differences between Li-ion diffusion in amorphous and crystalline Si as well as compare our results with past studies based on other methods.
© 2015 Elsevier Ltd. All rights reserved.

1. Introduction

Rechargeable Li-ion batteries are a critical part of the future energy storage needs in a broad range of applications: portable electronics, transport, power grid among others (Liu et al., 2012; Kasavajjula et al., 2007). Intense research is currently focused on understanding the basic materials science underscoring these energy storage devices to achieve high energy density storage and to mitigate the loss of capacity due to chemical and mechanical degradation (Winter and Besenhard, 1999; Liu et al., 2012; Kasavajjula et al., 2007). Silicon (Si) is one of key materials being pursued for consideration as an anode material (Bucci et al., 2014). The ensuing (theoretical) charge capacity is more than an order of magnitude higher than carbon-based anodes (Winter and Besenhard, 1999; Sharma and Seefurth, 1976; Boukamp et al., 1981). During the charging and discharging process, Li-ions migrate from one electrode via the intervening electrolyte and insert and diffuse in the opposite electrode. Due to the high Li capacity of the Si anode, the insertion and diffusion of Li ions is accompanied with a rather large (nearly four-fold) volumetric swelling and the consequent generation of mechanical stresses. Fracture, loss of structural integrity and the irreversible capacity loss that consequently follow are mainly attributed to swelling induced mechanical stresses (Kim et al., 2014; Zhao et al., 2010). Significant loss of capacity is often seen after only a few charge–discharge cycles (Hatchard and Dahn, 2004).

The use of amorphous silicon (a-Si), instead of its crystalline counterpart, is considered to offer several advantages. Experiments have shown that the amorphous

* Corresponding author at: Department of Mechanical Engineering, University of Houston, Houston, TX 77004, USA.
E-mail address: psharma@uh.edu (P. Sharma).

http://dx.doi.org/10.1016/j.mechmat.2015.04.001
0167-6636/© 2015 Elsevier Ltd. All rights reserved.

Please cite this article in press as: Yan, X., et al. Atomistic insights into Li-ion diffusion in amorphous silicon. Mech. Mater. (2015), http://dx.doi.org/10.1016/j.mechmat.2015.04.001

alloys tend to cycle better than the corresponding crystalline phases (Beaulieu et al., 2001; Beaulieu et al., 2003a,b). These works have concluded that the mechanisms underlying loss of capacity in amorphous anode materials is different than from the crystalline phases. In crystals, following lithium insertion, intermetallic phases are formed that induce inhomogeneous volume expansion and cracking. Although the lithiation induced volume expansion is found to be larger in amorphous materials (Zhao et al., 2010), the deformation is *homogeneous*, and *reversible*; in sharp contrast to the crystalline phase behavior (Beaulieu et al., 2001; Beaulieu et al., 2003a). Finally, c-Si converts to an amorphous Li–Si alloy phase during lithiation (Limthongkul et al., 2003b,a; Chan et al., 2007) which generates additional mechanical stresses that accompany the phase transition process (Zhao et al., 2010). In summary, there are several technologically relevant reasons to consider a-Si as a viable alternative to c-Si.

The atomistic mechanisms underpinning diffusive transport of Li-ions in a-Si are, however, not fully understood. Experimental studies of Li diffusion in a-Si matrix reveal a wide scatter in the diffusion constant: 1×10^{-10} to 1×10^{-14} cm^2 s^{-1} (Ding et al., 2009; Xie et al., 2010; Yoshimura et al., 2007). The reported results are for diffusion of multiple Li-ion atoms. While more realistic, this prevents a "clean" understanding of the single Li-ion diffusion mechanism. A potential recourse is to use atomistic simulations to obtain the requisite insights. One such study was performed by Tritsaris et al. (2012) which yielded several interesting insights. Density Functional Theory (DFT) based calculations were used to study the single Li-ion diffusion mechanism by postulating predetermined Li-atom positions and diffusive pathways. They concluded that the rate of long-range Li diffusion in a-Si is comparable to the rate in c-Si. One of the limitations of the aforementioned study is that the Li-atom sites and diffusion pathways were *pre-determined*—based on physical intuition. There is no guarantee that those pre-set pathways are the actual (or the most probable) pathways. Alternatively, if one is willing to use empirical force-fields, conventional molecular dynamics (MD) may be used to address this problem. However, as is well known, classical MD (usually) can only handle time-scales of a few hundred to thousand nanoseconds (Nielsen et al., 2010). Thus for slow processes, such as diffusion and creep, conventional MD is clearly not the best choice. In the present context, MD will fail to account for diffusion pathways that have relaxation times longer than hundred of nanoseconds.

In this work, we employ a sequence of methods to perform, at least from the time-scale viewpoint, realistic simulations that provide insights into Li -ion diffusion in both a-Si and c-Si. Our work is based on the recent success of a potential energy surface sampling approach—the so-called autonomous basin climbing (ABC) algorithm (Kushima et al., 2009; Lau et al., 2010; Fan et al., 2011)). Our study adopts a similar *starting* point as Tritsaris et al. (2012), however, instead we employ the ABC approach for potential energy sampling, and then in conjunction with kinetic Monte Carlo (KMC) and transition state theory (TST), we determine the most probable diffusion pathways and kinetics for a single Li atom in both a-Si and c-Si.

2. Approach and simulation details

An overview of our overall computational approach is depicted in Fig. 1. Below, we briefly describe the four steps (Fig. 1a–d) of our approach: (1) For a given set of boundary conditions, the ABC method is used to sample the potential

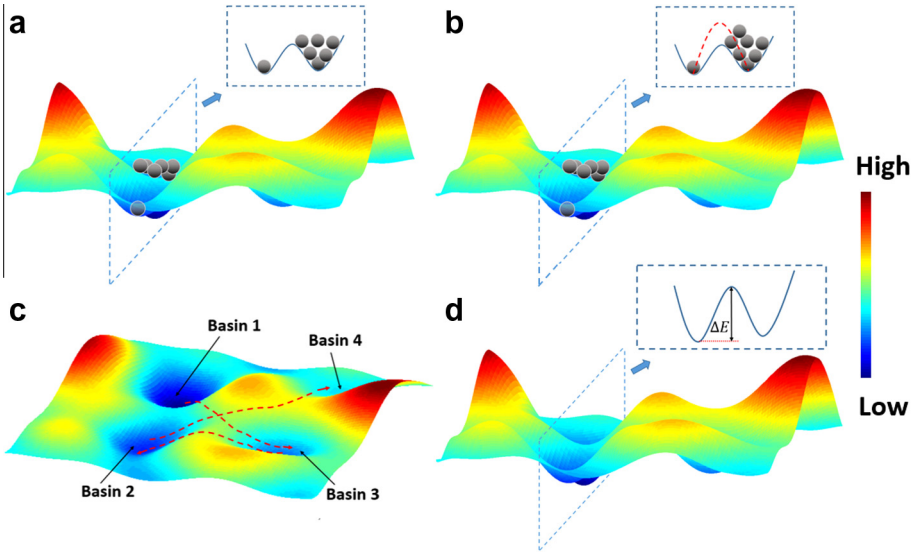

Fig. 1. Illustration of the computational approach: (a) ABC algorithm—the potential energy surface is unknown *a priori* and this figure is merely a schematic of complex 3N-dimensional PES; the black balls represent the penalties added to the system; (b) The barriers estimated in ABC, red dashed curve, are usually higher than the actual barriers, although the minima are correctly estimated. The NEB approach is used to refine the calculation of the energy barrier; (c) The basins 1–4 are discovered in ABC. KMC then allows the determination of the most probable pathway e.g. as an example shown in the figure, 1–3–2–4; (d) barrier energy ΔE is used in TST to calculate the rate constant for KMC and the transition time of every step after KMC. (For interpretation of the references to colour in this figure caption, the reader is referred to the web version of this article.)

Please cite this article in press as: Yan, X., et al. Atomistic insights into Li-ion diffusion in amorphous silicon. Mech. Mater. (2015), http://dx.doi.org/10.1016/j.mechmat.2015.04.001

energy surface (PES)—this determines the minima of the PES as well as the saddle points yielding thus the energy barriers between different local minima (Fig. 1a). The 3N-dimensional PES is quite complex indeed and Fig. 1a is merely schematic representation to provide intuition to the reader. (2) As will be explained further in the next few paragraphs, the energy barriers obtained from ABC are approximate since the determination of the saddle points can be in error based on the resolution of the sampling approach. Accordingly, to extract accurate energy barriers, the nudged elastic band method (NEB) is applied to *all* the minima pairs that are obtained from the ABC algorithm (Fig. 1b). This is a fairly tedious step e.g. if only 10 minima are identified by ABC, a 10×10 matrix of energy-barrier pairs needs to be calculated. (3) With the energy barriers in hand, KMC is used to find the most probable pathway between the different PES minima (Fig. 1c). (4) Following the pathway provided in step (3), TST is used to calculate the transition time between two steps (3). The time information is combined with mean square displacement between the two steps to extract the diffusivity.

Inspired by the time-scaling approach of metadynamics (Laio and Gervasio, 2008) the ABC algorithm was developed by Kushima, Yip and co-workers (Lau et al., 2010; Kushima et al., 2009; Kushima et al., 2011). In this approach, an energy minimized initial structure is activated by adding a penalty energy $\Phi_p^k(r)$ followed by a subsequent relaxation. The penalty energy is in the form of a 3N gaussian penalty function:

$$\Phi_p^k(r) = \omega exp\left[-(r - r_{min}^k)/2\sigma^2\right] \quad (1)$$

centered at the minimum configuration r_{min}^k. The parameters ω and σ control the shape of the penalty function. Through repeated application of the penalty imposition and the relaxation process, the system is pushed to climb up the basin to a higher energy configuration. In this manner, the algorithm outputs the configurations that the system visits successively, moving from one energy basin to another through energy activation and relaxation steps as shown in Fig. 1a. We have implemented a parallel version of this algorithm in the LAMMPS software (Plimpton, 1995). The size of the penalty should not be too large so that physically meaningful potential wells are not missed, nor too small that too many iterations are required to climb the barriers and obtain a *reasonable* sampling of the PES. Further details can be found in the following papers: (Lau et al., 2010; Kushima et al., 2009; Kushima et al., 2011). Needless to say, the sampling of a system of even a few thousand atoms is computationally demanding. Recently, a rather interesting approach has been taken by Park and co-workers (Cao et al., 2012, 2014), who have modified the ABC approach so that the system adapts the penalty function parameters through a *self-learning* process.

With a suitable penalty size and long-enough sampling time, in principle, the ABC algorithm can provide a "reasonable" approximation of the PES. Although the local minima are indeed captured accurately, unless the penalties are very small, the energy barriers are overestimated (Fig. 1b red dash curve). Thus, to improve the accuracy of the energy barrier estimates, smaller penalties should be applied. However, this strategy is accompanied by a significant computational cost. Alternatively, the NEB (Henkelman and Jonsson, 2000; Henkelman et al., 2000) method can be applied to the output of the ABC to obtain accurate energy barriers between the various minima (Fig. 1b).

In ABC sampling, the sequence of the identified local minima is physically irrelevant. For example, starting from the same initial configuration, a different ABC computation (with a different set of parameters) may identify a different sequence of the minima. To ascertain the most probable pathway that the system follows in going from one physical state to the other, we use KMC (Voter, 2007). This method is used to calculate the corresponding possibilities for the system to cross every barrier (that has been identified) and to determine the most probable sequence for the system to cross the various energy barriers (Fig. 1c). With all the barrier information calculated from NEB, the transition state theory is then applied to estimate the rate constant (Fig. 1d) for each event (crossing a barrier):

$$k_{ij} \propto exp[-\Delta E/k_b T] \quad (2)$$

where k_{ij} is the rate constant for the single event, ΔE is the barrier energy calculated from ABC/NEB, k_b is Boltzmann constant and T is temperature. The rate constant divided by the summation of the rate constants of all possible events from the current state, yields the possibility of this single event. One of the possible transition is randomly chosen based on the relative possibilities. This is accomplished by comparing a randomly generated number in the range of (0,1] to an array of partial summation of the possibilities (Fig. 2). Starting from the new state, with the corresponding rate constants in the rate matrix, the same action is taken to find the next transition state (Fig. 2).

The simulation configuration chosen in this work is as follows. Fig. 3a and b show, respectively, the initial configurations for single Li-atom diffusion in a-Si and c-Si. The a-Si has 64 Si atoms—consistent with (Tritsaris et al., 2012), to facilitate a subsequent comparison. To ensure meaningful comparison between the crystalline and amorphous configurations, the former has an identical ratio of the number of Si–Li atoms. The size of crystalline matrix is 10.887 Å × 10.887 Å × 10.887 Å. Two of the Si atoms are fixed to avoid rotation and translation in all directions, and periodic boundary conditions are applied to both systems. The atomistic force-field used in this work is the Modified Embedded Atom Method (MEAM) potential developed by Cui et al. (2012).

The systems, crystalline and amorphous, are first equilibrated at 300 K under NVT condition to ensure that the Li atoms occupy the energetically optimal site in the Si-matrix. ABC sampling is initiated from these initial configurations.

3. Results and discussion

As alluded to earlier, in this study, we restrict our attention to monitoring the diffusion of a single Li atom in both crystalline and amorphous Si. We first discuss results for c-

Please cite this article in press as: Yan, X., et al. Atomistic insights into Li-ion diffusion in amorphous silicon. Mech. Mater. (2015), http://dx.doi.org/10.1016/j.mechmat.2015.04.001

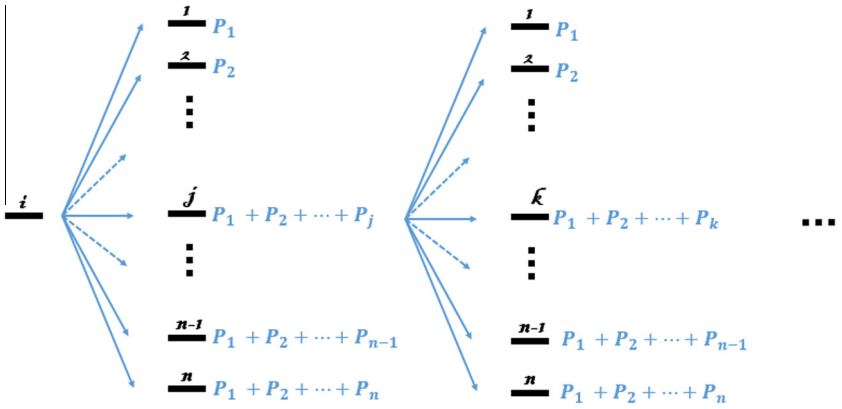

Fig. 2. KMC algorithm: Starting from the *i*th state, a random number (r) in the range of (0,1] is compared with the partial summation of possibilities: $P_1 + P_2 + \ldots + P_{j-1} < r < P_1 + P_2 + \ldots + P_j$. The system will jump to state *j*. State *j* becomes then the current state and same process is re-initiated from state *j*.

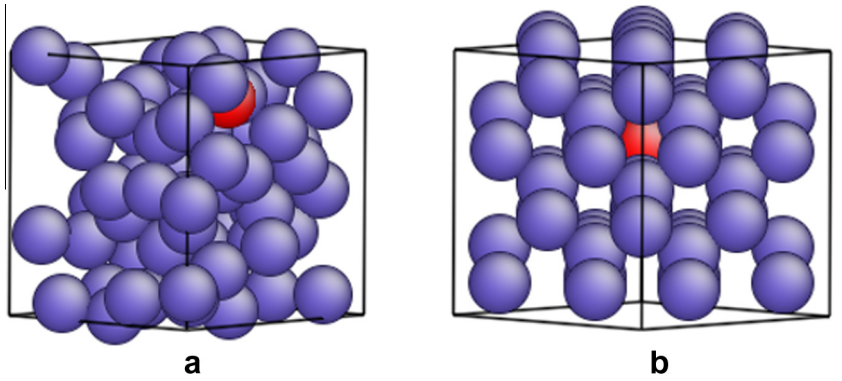

Fig. 3. Initial simulation structure of Li diffusion in amorphous (a) and crystalline (b) silicon matrix.

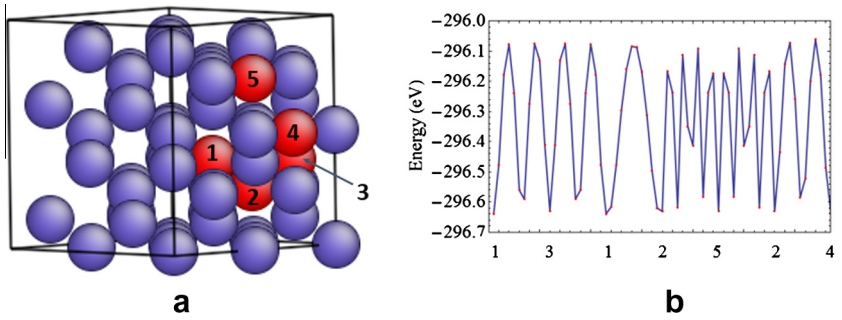

Fig. 4. Diffusion path and corresponding barriers of single Li diffusion in crystalline Si matrix. (For interpretation of the references to colour in this figure caption, the reader is referred to the web version of this article.)

Si. For this particular case, we do not expect our results to differ from other approaches and accordingly, this is a useful benchmark analysis. For the Li-atom diffusion in the crystalline matrix, as shown in Fig. 4a, the captured possible Li sites are shown in red. The numbers on the atoms indicate the sequence of the sites captured in ABC. It is observed that all the possible Li sites are in the T_d positions which is consistent with Tritsaris' work (Tritsaris et al., 2012). The T_d site lies at a distance of b_o away from a Si atom in the direction opposite from one of its nearest neighbor Si atoms (b_o equals to the bond length of crystalline silicon matrix). The diffusion pathways and the energy barriers that are obtained from KMC are shown in Fig. 4b. The barriers between two sites are around 0.5 eV which is also consistent with the results reported by Tritsaris et al. (2012) and the corresponding diffusion coefficient of 5.01×10^{-12} cm^2 s^{-1} agrees with the results in the literature. Based on this comparison, we conclude that

Please cite this article in press as: Yan, X., et al. Atomistic insights into Li-ion diffusion in amorphous silicon. Mech. Mater. (2015), http://dx.doi.org/10.1016/j.mechmat.2015.04.001

the present method can reasonably capture Li diffusion in c-Si. In the following, we discuss our results for a-Si—the main focus of this work.

For the amorphous system, different penalty size is used with $\omega = 2$ and $\sigma = 2$. After ABC calculations for Li in a-Si, a total of 260 minima are sampled. Among all these configurations, if any two states have Li-atoms positions that differ by <0.6 Å *and* if the energy barrier between those two states is less than the thermal fluctuation ($k_bT \approx 0.026$ eV), we consider them to be in the same potential well and one of them is removed from the minima list. After this paring down, 3 local minima are eliminated. NEB calculation is then carried out to provide a 257×257 barrier matrix which contains energy barrier between all the pairs. KMC algorithm is applied to find the most probable diffusive pathway. Unlike the crystalline case, the diffusion pathway and kinetics is strongly dependent on the initial site of the Li-atom diffusion. To obtained a deeper understanding of this, we carried out 257 KMC simulations starting from different basins and distinguish four scenarios:

(1) Scenario 1: Li atom diffuses a few steps and gets trapped in some wells—subsequently then shuttling back and forth among two or more wells. The reason for this phenomenon is that the barriers between these wells and other "outside wells" are significantly higher and the chances for the Li atom to diffuse out of the traps are low. Taking the states 129 and 130 as an example, in Fig. 5a and b, the Li atom diffuses back and forth in these two sites, and the diffusion distance of Li atom is 2.03 Å. The corresponding barriers are shown in Fig. 5c and d with the value of 0.113 eV and 0.649 eV. Except for the barriers between state 129 and 130, the smallest barrier starting from states 129 and 130 are 2.606 eV and 2.211 eV. Applying Eq. (2), it is found that the rate constant for barrier between state 129 and 130 are 0.013 and 3.11×10^{-11}, and the rate constant for the smallest "outside barrier" are 2.9×10^{-44} and 1.17×10^{-37}.
(2) Scenario 2: The Li atom is trapped between some wells but then after some iterations, is able to move to other basins.
(3) Scenario 3: The initial site is a "dead" site. By "dead site", here, we mean that the barriers from this site to others are higher than 1.2 eV which indicates that at room temperature (300 K), the system requires longer than half a year to diffuse out of this well and the time it requires is much longer than usual charging and discharging time. Thus, we assume that if the barrier is larger than 1.2 eV, diffusion rate is slow enough to be physically irrelevant.
(4) Scenario 4: After a very short diffusive path, the Li atom ends up in a dead site. This case is also pointed out in the work of Tritsaris et al. (2012), however their approach precludes the determination of the actual pathways.

To calculate the diffusion coefficient, we find the gradient of mean square displacement (R^2) versus time t and using the Einstein relation

$$D = \lim_{t\to\infty}(R_j - R_i)^2/6t \tag{3}$$

The time t, is obtained from the transition state theory

$$t_{i-j} = (\nu exp[-\Delta E_{i-j}/k_bT])^{-1}. \tag{4}$$

where ν is the hopping frequency taken to be $10^{13}s^{-1}$. For scenario (1) and scenario (2), the diffusion coefficient is obtained based on 100 KMC iterations. For scenario (3), we assume that the diffusion will not happen. For scenario (4), we only collect data until the Li-atom diffuses to a

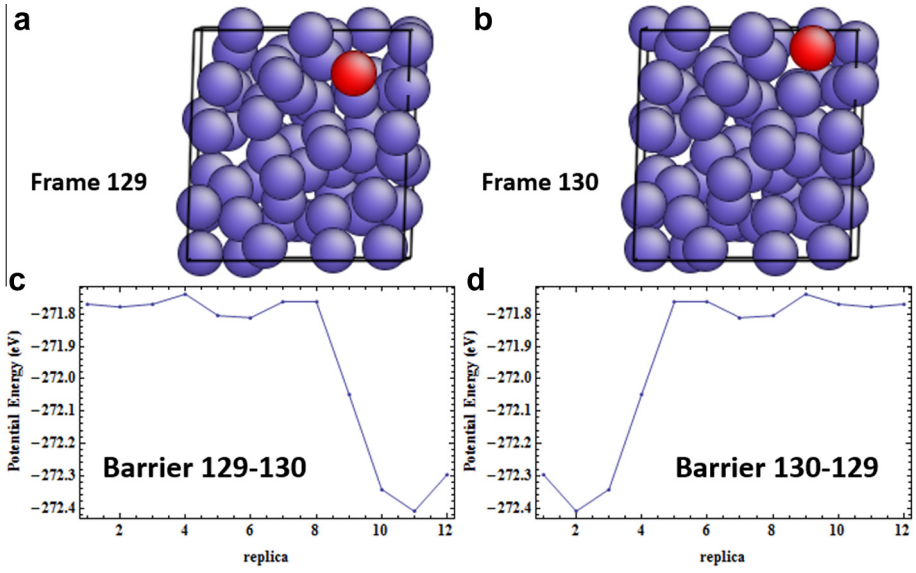

Fig. 5. (a) Configuration of frame 129; (b) configuration of frame 130; (c) NEB results of barrier from frame 129 to frame 130; (d) NEB results of barrier from frame 130 to frame 129.

Please cite this article in press as: Yan, X., et al. Atomistic insights into Li-ion diffusion in amorphous silicon. Mech. Mater. (2015), http://dx.doi.org/10.1016/j.mechmat.2015.04.001

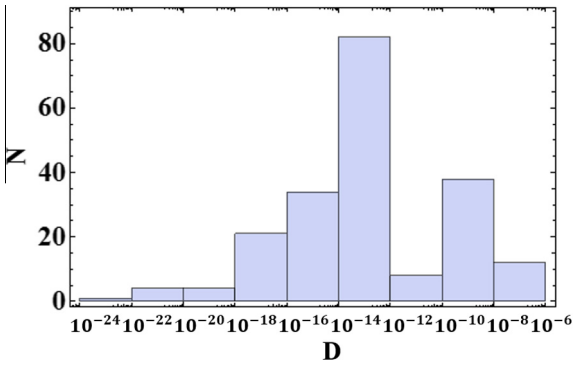

Fig. 6. Distribution of diffusivities after KMC calculation.

dead-site. As a result, 204 diffusion coefficients (obtained from different initial sites) are shown in Fig. 6. As is evident from Fig. 6, the estimated diffusion coefficient exhibits a wide range of values: from 10^{-24} cm^2 s^{-1} to 10^{-6} cm^2 s^{-1}. However, the preponderance of the distribution (around 80%) is in the range of 10^{-16} to 10^{-8} cm^2 s^{-1}. This range is a little bit larger than what has been reported in experiments: (10^{-14} to 10^{-10} cm^2 s^{-1}), and the possible reason is that in this work, we have focused on the diffusion of single Li atom as opposed to diffusion of multiple Li-atoms. It is worth emphasizing that, in Fig. 6, the slower diffusion rates cannot be captured by *conventional* molecular dynamics.

4. Summary

Understanding the kinetics of diffusive transport of Li atoms in amorphous silicon is an important first step to establish the relevant materials science for potential application of this material as an anode in Lithium-ion batteries. The traditional atomistic approaches suffer from various limitations when dealing with physical phenomena that involve relaxation times longer than hundreds of nanoseconds and/or complex materials (such as amorphous) where reaction pathways are not necessarily intuitively obvious. In this work, we concoct together a series of computational atomistic approaches, the so-called autonomous basic climbing algorithm that allows potential energy landscape sampling, nudged elastic band, kinetic Monte Carlo and finally transition state theory to obtain insights into Li diffusion in amorphous silicon. The probable diffusive pathways naturally emerge from our approach and we are able to replicate the diversity of diffusivities obtained in experiments. The presented work, potentially, paves the way for *materials design* using the approach described herein.

Acknowledgements

The research was partially supported by AFOSR grant AFOSR FA9550–09-1–0200, the University of Houston and the M.D. Anderson Professorship.

References

Beaulieu, L., Eberman, K., Turner, R., Krause, L., Dahn, J., 2001. Colossal reversible volume changes in lithium alloys. Electrochem. Solid State Lett. 4, A137–A140.
Beaulieu, L., Hatchard, T., Bonakdarpour, A., Fleischauer, M., Dahn, J., 2003a. Reaction of Li with alloy thin films studied by in situ AFM. J. Electrochem. Soc. 150, A1457–A1464.
Beaulieu, L., Hewitt, K., Turner, R., Bonakdarpour, A., Abdo, A., Christensen, L., Eberman, K., Krause, L., Dahn, J., 2003b. The electrochemical reaction of Li with amorphous Si–Sn alloys. J. Electrochem. Soc. 150, A149–A156.
Boukamp, B., Lesh, G., Huggins, R., 1981. All-solid lithium electrodes with mixed-conductor matrix. J. Electrochem. Soc. 128, 725–729.
Bucci, G., Nadimpalli, S.P., Sethuraman, V.A., Bower, A.F., Guduru, P.R., 2014. Measurement and modeling of the mechanical and electrochemical response of amorphous Si thin film electrodes during cyclic lithiation. J. Mech. Phys. Solids 62, 276–294.
Cao, P., Li, M., Heugle, R.J., Park, H.S., Lin, X., 2012. Self-learning metabasin escape algorithm for supercooled liquids. Phys. Rev. E 86, 016710.
Cao, P., Lin, X., Park, H.S., 2014. Strain-rate and temperature dependence of yield stress of amorphous solids via a self-learning metabasin escape algorithm. J. Mech. Phys. Solids 68, 239–250.
Chan, C.K., Peng, H., Liu, G., McIlwrath, K., Zhang, X.F., Huggins, R.A., Cui, Y., 2007. High-performance lithium battery anodes using silicon nanowires. Nat. Nanotechnol. 3, 31–35.
Cui, Z., Gao, F., Cui, Z., Qu, J., 2012. A second nearest-neighbor embedded atom method interatomic potential for Li–Si alloys. J. Power Sources 207, 150–159.
Ding, N., Xu, J., Yao, Y., Wegner, G., Fang, X., Chen, C., Lieberwirth, I., 2009. Determination of the diffusion coefficient of lithium ions in nano-Si. Solid State Ionics 180, 222–225.
Fan, Y., Kushima, A., Yip, S., Yildiz, B., 2011. Mechanism of void nucleation and growth in bcc Fe: atomistic simulations at experimental time scales. Phys. Rev. Lett. 106, 125501.
Hatchard, T., Dahn, J., 2004. In situ XRD and electrochemical study of the reaction of lithium with amorphous silicon. J. Electrochem. Soc. 151, A838–A842.
Henkelman, G., Jonsson, H., 2000. Improved tangent estimate in the nudged elastic band method for finding minimum energy paths and saddle points. J. Chem. Phys. 113, 9978–9985.
Henkelman, G., Uberuaga, B.P., Jónsson, H., 2000. A climbing image nudged elastic band method for finding saddle points and minimum energy paths. J. Chem. Phys. 113, 9901–9904.
Kasavajjula, U., Wang, C., Appleby, A.J., 2007. Nano-and bulk-silicon-based insertion anodes for lithium-ion secondary cells. J. Power Sources 163, 1003–1039.
Kim, S.P., Datta, D., Shenoy, V.B., 2014. Atomistic mechanisms of phase boundary evolution during initial lithiation of crystalline silicon. J. Phys. Chem. C 118, 17247–17253.
Kushima, A., Eapen, J., Li, J., Yip, S., Zhu, T., 2011. Time scale bridging in atomistic simulation of slow dynamics: viscous relaxation and defect activation. Eur. Phys. J. B: Condens. Matter Complex Syst. 82, 271–293.
Kushima, A., Lin, X., Li, J., Eapen, J., Mauro, J.C., Qian, X., Diep, P., Yip, S., 2009. Computing the viscosity of supercooled liquids. J. Chem. Phys. 130, 224504.
Laio, A., Gervasio, F.L., 2008. Metadynamics: a method to simulate rare events and reconstruct the free energy in biophysics, chemistry and material science. Rep. Prog. Phys. 71, 126601.
Lau, T.T., Kushima, A., Yip, S., 2010. Atomistic simulation of creep in a nanocrystal. Phys. Rev. Lett. 104, 175501.
Limthongkul, P., Jang, Y.I., Dudney, N.J., Chiang, Y.M., 2003a. Electrochemically-driven solid-state amorphization in lithium–metal anodes. J. Power Sources 119, 604–609.
Limthongkul, P., Jang, Y.I., Dudney, N.J., Chiang, Y.M., 2003b. Electrochemically-driven solid-state amorphization in lithium-silicon alloys and implications for lithium storage. Acta Mater. 51, 1103–1113.
Liu, X.H., Zhong, L., Huang, S., Mao, S.X., Zhu, T., Huang, J.Y., 2012. Size-dependent fracture of silicon nanoparticles during lithiation. ACS Nano 6, 1522–1531.
Nielsen, S.O., Bulo, R.E., Moore, P.B., Ensing, B., 2010. Recent progress in adaptive multiscale molecular dynamics simulations of soft matter. Phys. Chem. Chem. Phys. 12, 12401–12414.
Plimpton, S., 1995. Fast parallel algorithms for short-range molecular dynamics. J. Comput. Phys. 117, 1–19.
Sharma, R.A., Seefurth, R.N., 1976. Thermodynamic properties of the lithium-silicon system. J. Electrochem. Soc. 123, 1763–1768.

Please cite this article in press as: Yan, X., et al. Atomistic insights into Li-ion diffusion in amorphous silicon. Mech. Mater. (2015), http://dx.doi.org/10.1016/j.mechmat.2015.04.001

Tritsaris, G.A., Zhao, K., Okeke, O.U., Kaxiras, E., 2012. Diffusion of lithium in bulk amorphous silicon: a theoretical study. J. Phys. Chem. C 116, 22212–22216.

Voter, A., 2007. Introduction to the kinetic Monte Carlo method. In: Sickafus, K., Kotomin, E., Uberuaga, B. (Eds.), Radiation Effects in Solids, NATO Science Series, vol. 235, pp. 1–23.

Winter, M., Besenhard, J.O., 1999. Electrochemical lithiation of tin and tin-based intermetallics and composites. Electrochim. Acta 45, 31–50.

Xie, J., Imanishi, N., Zhang, T., Hirano, A., Takeda, Y., Yamamoto, O., 2010. Li-ion diffusion in amorphous Si films prepared by RF magnetron sputtering: a comparison of using liquid and polymer electrolytes. Mater. Chem. Phys. 120, 421–425.

Yoshimura, K., Suzuki, J., Sekine, K., Takamura, T., 2007. Measurement of the diffusion rate of Li in silicon by the use of bipolar cells. J. Power Sources 174, 653–657.

Zhao, K., Pharr, M., Vlassak, J.J., Suo, Z., 2010. Fracture of electrodes in lithium-ion batteries caused by fast charging. J. Appl. Phys. 108, 073517.

Please cite this article in press as: Yan, X., et al. Atomistic insights into Li-ion diffusion in amorphous silicon. Mech. Mater. (2015), http://dx.doi.org/10.1016/j.mechmat.2015.04.001